Rapid Report

Spark- and ember-like elementary Ca^{2+} release events in skinned fibres of adult mammalian skeletal muscle

Wolfgang G. Kirsch, Dietmar Uttenweiler and Rainer H. A. Fink

Institute of Physiology and Pathophysiology, Medical Biophysics, University of Heidelberg, Im Neuenheimer Feld 326, 69120 Heidelberg, Germany

(Resubmitted 27 August 2001; accepted after revision 15 October 2001)

1. Using laser scanning confocal microscopy, we show for the first time elementary Ca^{2+} release events (ECRE) from the sarcoplasmic reticulum in chemically and mechanically skinned fibres from adult mammalian muscle and compare them with ECRE from amphibian skinned fibres.
2. Hundreds of spontaneously occurring events could be measured from individual single skinned mammalian fibres. In addition to spark-like events, we found ember-like events, i.e. long-lasting events of steady amplitude. These two different fundamental release types in mammalian muscle could occur in combination at the same location.
3. The two peaks of the frequency of occurrence for ECRE of mammalian skeletal muscle coincided with the expected locations of the transverse tubular system within the sarcomere, suggesting that ECRE mainly originate at triadic junctions.
4. ECRE in adult mammalian muscle could also be identified at the onset of the global Ca^{2+} release evoked by membrane depolarisation in mechanically skinned fibres. In addition, the frequency of ECRE was significantly increased by application of 0.5 mM caffeine and reduced by application of 2 mM tetracaine.
5. We conclude that the excitation–contraction coupling process in adult mammalian muscle involves the activation of both spark- and ember-like elementary Ca^{2+} release events.

Ca^{2+} release from the sarcoplasmic reticulum (SR) in skeletal muscle through single or clusters of ion channels of the ryanodine receptor (RYR) family occurs mainly at triadic junctions (Dulhunty, 1992; Escobar *et al.* 1994). At these junctions, the membranes of the transverse tubular system (TTS) and the SR, in close proximity, allow the formation of assemblies of RYRs and voltage-sensing dihydropyridine receptors (DHPRs). The pattern of this assembly suggests that there is more than one control mechanism for Ca^{2+} release. Every other receptor in the double row of RYRs is colocalised with tetrads of DHPRs (skip pattern; Block *et al.* 1988), enabling the triggering of Ca^{2+} release by protein–protein interactions upon changes in transverse tubular membrane potential (Ríos & Brum, 1987). In addition, the activation of RYRs alone is modulated by a large variety of physiologically important factors, e.g. the cytosolic free Ca^{2+} or Mg^{2+} concentration (Franzini-Armstrong & Protasi, 1997; Lamb, 2000), the redox state (e.g. Haarmann *et al.* 1999) or cytostructural proteins (Franzini-Armstrong & Protasi, 1997; Balshaw *et al.* 2001).

Due to their brevity, the first detected elementary Ca^{2+} release events (ECRE) of excitation–contraction coupling (E–C coupling) were termed Ca^{2+} sparks in heart (Cheng *et al.* 1993), and in amphibian skeletal (Tsugorka *et al.* 1995; Klein *et al.* 1996) and smooth muscle (Nelson *et al.* 1995). The so-called Ca^{2+}-induced Ca^{2+} release (CICR), the main trigger for these events in heart muscle (Lipp & Niggli, 1998), appears to be involved in Ca^{2+} sparks in amphibian skeletal muscle (Klein *et al.* 1996; González *et al.* 2000*a*,*b*), where sparks can also be induced by depolarisation of the transverse tubular membrane. Embers, long-duration low fluorescence intensity prolongations at the spatial core of individual Ca^{2+} sparks or Ca^{2+} spark averages, have recently been reported in amphibian skeletal muscle and are interpreted as a manifestation of Ca^{2+} release directly operated by voltage sensors (González *et al.* 2000*b*).

Although Ca^{2+} sparks have been found in developing mammalian muscle (Shirokova *et al.* 1999; Conklin *et al.* 2000; Ward *et al.* 2000), to date the existence and physiological role of ECRE in adult mammalian muscle remains controversial, with results ranging from non-existant, from voltage-clamp studies on adult rat muscle (Shirokova *et al.* 1998), to only a scarce appearance of spontaneous Ca^{2+} sparks in intact adult mouse muscle fibres (Conklin *et al.* 1999). The present study addresses

this controversy in adult mammalian skeletal muscle and shows the existence of two types of ECRE, spark- and ember-like events, which may be essential for Ca^{2+} release in mammalian E–C coupling.

METHODS

Fibre preparation

All animals were handled according to the guidelines of the animal care committee of the University of Heidelberg. Balb/C mice and Wistar rats (both 12–16 weeks old) were killed by exposure to a rising concentration of CO_2. Frogs (*Xenopus laevis*) were killed by decapitation and subsequent double-pithing after being deeply anaesthetised in a 15% ethanol–water solution.

Single fibres from the tibialis anticus muscle of the frog were used for the chemically skinned amphibian fibre preparations. For skinned mammalian fibre preparations, single fibres from the extensor digitorum longus (EDL) muscle of male mice and rats were used. All muscles were stored in standard Ringer or Krebs-Ringer solution prior to dissection of single fibres. First, bundles of 10–20 fibres were cut and gently dissected with forceps from the complete muscles, which were fixed with syringe needles to Sylgard-coated Petri dishes and bathed in the respective relaxing solution. From these bundles, again fixed with 'insect' needles to the Petri dish, single fibres were dissected under gentle stretch. Only fibres that remained slack at the bottom of the Petri dish after the dissection procedure were used for experiments. During mechanical skinning (e.g. Fink & Stephenson, 1987) the individual fibres remained immersed in the respective relaxing solution. The single fibres, always covered with solution, were then transported using an adjusted plastic pipette tip to the experimental chamber, which was filled with relaxing solution. The ends of the single fibres were fixed with Scotch tape to areas, which were covered with Glisseal (Borer Chemie, Zuchwil, Switzerland), on the glass coverslip bottom of the chamber. For chemically skinned fibres, permeabilisation was achieved inside the experimental chamber by a 2 min exposure to 0.01% saponin in relaxing solution. The saponin-containing relaxing solution was carefully washed out of the chamber with the respective internal solution (not containing Fluo-4). Eventually, in all cases, the fibres were bathed in the respective internal solution containing 60 μM Fluo-4. Sarcomere lengths, determined from the regular striated pattern of amphibian and mammalian fibres in images obtained with the transmission detector of the confocal microscope, varied between 2.2 and 3 μm.

Fluorescence imaging

The experimental chamber was mounted on an inverted microscope (IX70, Olympus) and fibres were imaged through a ×40 water-immersion objective (UAPO40×W/340/1.15, Olympus) with a confocal laser scanning unit (FV-300, Olympus) using the 488 nm line of a 20 mW Kr/Ar-laser (Omnichrome, Melles Griot). For all experiments the laser was attenuated to 6% with a neutral density filter. The fluorescence emission was measured at wavelengths greater than 510 nm using a barrier filter and a pinhole size of 150 μm. The photomultiplier output was digitised with 12 bit resolution. The dimensions for the x–y images were 512 pixels × 512 pixels, where the pixel size was 0.1365 μm in both the x- and y-direction and when consecutive x–y images (xyt-series) were recorded the time interval between successive images was 2 s. xyt-series always contained 50 or 100 images and the individual images were taken at the same location inside the fibre. Linescan (x–t) images were obtained with 512 pixels (0.1365 μm per pixel) in the x- and 1000 pixels (2.05 ms per line) in the t-direction. We found no evidence for photodamage during the respective recording procedures nor was the occurrence of spark- or ember-like events dependent on the scanning time at a certain location under our conditions. The point spread function (PSF) of the confocal system was experimentally determined using subresolution fluorescent beads (TetraSpeck, Molecular Probes) with a diameter of 100 nm. The lateral and axial resolutions for the experimental settings described above were 0.35 ± 0.02 and 1.06 ± 0.05 μm, respectively. The resolution was determined from the full-width at half-maximum (FWHM) of Gaussian fits applied to the lateral and axial intensity profiles of the subresolution beads imaged in xyz stacks.

As this is the first report on ECRE in skinned fibres of adult mammalian muscle, control experiments were carried out using a spectral confocal microscope (TCS-SP, Leica) that allowed a higher time resolution during line scanning (1.25 ms per line). The Leica set-up was based on an inverted microscope (DM IRB, Leica) with a ×63 water-immersion objective (PLAPO 63×/1.2W, Leica). No significant differences between the results obtained with the two set-ups could be observed.

Solutions

Solutions used were as follows. Amphibian relaxing solution (mM): 120 potassium glutamate, 10 Hepes, 5 glucose, 1 EGTA, 2 $MgCl_2$, pH 7.0; mammalian relaxing solution (mM): 140 potassium glutamate, 10 Hepes, 5 glucose, 1 EGTA, 10 $MgCl_2$, 0.3 $CaCl_2$, pH 7.0; amphibian internal solution (mM): 110 caesium glutamate, 10 Hepes, 5 glucose, 1 EGTA, 5 Na_2ATP, 5 Na_2phosphocreatine, 4.5 $MgCl_2$, 0.25 $CaCl_2$, 0.06 Fluo-4, pH 7.0; mammalian internal solution (high K^+) (mM): 140 potassium glutamate, 10 Hepes, 5 glucose, 0.5 EGTA, 5 Na_2ATP, 5 Na_2phosphocreatine, 5.4 $MgCl_2$, 0.1 $CaCl_2$, 0.06 Fluo-4, pH 7.0; high-Na^+ solution (mM): 140 sodium glutamate, 10 Hepes, 5 glucose, 5 EGTA, 5 Na_2ATP, 5 Na_2phosphocreatine, 5.46 $MgCl_2$, 0.9 $CaCl_2$, 0.06 Fluo-4, pH 7.0. The free Ca^{2+} concentration of the amphibian and mammalian internal solutions, as well as that of the high-Na^+ solution, was between 85 and 110 nM. The free Mg^{2+} concentration of the amphibian internal solution was 0.4 mM. For variations of the free Mg^{2+} concentration in the above mammalian internal solution, which had a free Mg^{2+} concentration of 0.6 mM, only the amount of $MgCl_2$ was modified as follows: 4.6 mM $MgCl_2$ for 0.4 mM free Mg^{2+} and 6.7 mM $MgCl_2$ for 1.0 mM free Mg^{2+}. For the respective calculations of the resulting free and bound metals and ligands we utilised the software program REACT II (obtained from G. L. Smith, University of Glasgow, UK). In addition to standard dissociation constants (Smith & Martell, 1994), we used a dissociation constant of 106 mM (20 °C, pH 7.0) for the 1:1 binding of Mg^{2+} ions to glutamate obtained from calibrations (W. G. Kirsch, unpublished observation). All experiments were carried out at room temperature (22 °C).

Image analysis

Event counting in x–y images was independently carried out visually by two observers and subsequently averaged. The number of events per image was saved and used for the calculation of the standard error of the mean (S.E.M.) for the event frequency in xyt-series.

Individual ECRE in linescans were first selected by eye. Linescan images of normalised fluorescence were obtained as follows. The average baseline fluorescence ($F_0(x)$) was calculated by averaging the fluorescence of the raw image ($F(x,t)$) prior to the event in the direction of the t-coordinate for each value of the spatial coordinate x. Normalisation of the image area containing the ECRE was carried out by calculating the ratio of $F(x,t)$ to $F_0(x)$ for each value of the temporal coordinate t. The normalised fluorescence image area was subsequently spatially filtered with a kernel size of 3 pixels. From the filtered normalised fluorescence image containing the event, four morphological parameters were determined: (i) amplitude (F/F_0): maximum normalised fluorescence in the image area containing the event; (ii) full-duration at half-maximum (FDHM): time corresponding to the number of pixels greater than half-amplitude at the spatial coordinate containing the maximum amplitude; (iii) rise time:

calculated as the time elapsed between 10% and the peak of the amplitude; and (iv) full-width at half-maximum (FWHM): determined from the number of pixels greater than half-amplitude at the time of maximum amplitude.

In order to determine the position of the event maximum relative to the sarcomeric structure of skeletal muscle fibres, as shown in Fig. 1*C*, the positions of the maxima of the regular baseline fluorescence pattern prior to the event were first determined. The baseline fluorescence maxima were assumed to correspond to the middle of a sarcomere (as published in Klein *et al.* 1996; Shirokova *et al.* 1998). Therefore, the positions of the Z-lines were assumed to be located half-way between the baseline fluorescence maxima. Subsequently the relative distance (d), in units of fractions of a sarcomere, of the event maximum to the closest Z-line was calculated. Thus, d falls into the interval (0, 0.5). For better visualisation, the relative frequency of the positions relative to the Z-line in Fig. 1*C* is displayed from the middle of one sarcomere to the middle of the adjacent sarcomere. To achieve this the histogram for $0 < d < 0.5$ was mirrored at $d = 0$.

All digital image processing of the original TIFF files or BMP files saved by the Olympus Fluoview 3.0 software was carried out with self-written algorithms within the software environment IDL 5.4 (Interactive Data Language, Research Systems Inc.; distributed by CREASO, Gilching, Germany).

Statistical analysis

All data are presented as means ± S.E.M. Statistical analysis was carried out using the software package Sigma Plot 2000 (SPSS Inc., Chicago, USA). To test the significance of the effects of pharmacological agents or physiologically important factors on ECRE frequency, Student's t tests were applied and P values less than 0.05 were defined as significant.

RESULTS

We studied chemically (Uttenweiler *et al.* 1998) and mechanically (Fink & Stephenson, 1987) skinned fibres of adult mammalian skeletal muscle using confocal laser scanning microscopy in order to demonstrate and characterise ECRE in these preparations. As shown in Fig. 1*A*, chemically (*a*–*d*) and mechanically (*e*–*h*) skinned fibres from Balb/C mice exhibited about one to four events per x–y image in a time series of 100 images (70 × 70 μm^2; interval, 2 s). Similar event frequencies of ECRE were observed in chemically skinned fibres from Wistar rats (*k*–*n*), showing that the abundant occurrence of ECRE was independent of the skinning procedure or animal species under equivalent ionic conditions for the internal solution. All further results described in this study refer to mammalian skeletal muscle from Balb/C mice only or to skeletal muscle of *Xenopus laevis*, for comparison with amphibian muscle.

In linescans along the fibre axis (70 μm, 2 s), skinned mammalian fibres exhibited about one to three ECRE per image, as shown for a representative chemically skinned mammalian fibre in Fig. 1*Ba*. Over 100 individual events could be collected from a single skinned fibre, where fibres were usually observed for 0.5–1 h. The event frequency in chemically skinned fibres from frog was about 10 Ca^{2+} sparks per image under similar conditions, as shown for a representative fibre in Fig. 1*Bb*. The linescans clearly indicate that there are profound differences in the spatial and temporal properties of events (event morphology) between amphibian and adult mammalian muscle. To characterise the spatial and temporal properties of the ECRE four event parameters were quantified after normalisation to baseline fluorescence: amplitude (F/F_0), FWHM, FDHM and rise time, as described in Methods.

We also studied the location of the ECRE maximum relative to the sarcomeric structure of skeletal muscle. Figure 1*C* shows the frequency of occurrence of ECRE relative to the Z-line and the TTS in mammalian (*a*) and amphibian (*b*) muscle. The abscissa of the respective histogram corresponds to the relative distance from the Z-line. A schematic diagram of the regular molecular sarcomeric structure showing actin and myosin filaments, the Z-line and the location of the TTS for the respective species is shown above each histogram. Only events that occurred within a noticeable regular baseline pattern that could be attributed to the sarcomeric structure were used for the analysis. Figure 1*Ca* includes 127 events (all ECRE types) of a mechanically skinned mammalian fibre and Fig. 1*Cb* includes 131 events of a chemically skinned amphibian fibre. Unfortunately, chemically skinned mammalian fibres did not show sufficient regular baseline patterns, and therefore this type of analysis could not be carried out in these preparations. It became clear that ECRE mainly occurred close to the expected positions of the TTS, indicating that most of the observed events originate at the triadic junctions in both mammals and frogs. Thus, the ECRE observed in our study appear to directly reflect elementary signals relevant to the E–C coupling process in adult mammalian muscle.

Figure 2*A* shows representative examples of spontaneously occurring events in both resting mechanically and chemically skinned mammalian fibres studied using line scanning. Panels *a*–*c* depict events that showed a sharp rise in fluorescence from the baseline and a somewhat slower decay. The shape of the time course of these events was basically similar to that of Ca^{2+} sparks in amphibian muscle, although on average the durations of these spark-like ECRE were longer in mammalian fibres. A typical amphibian Ca^{2+} spark under our experimental conditions had a FDHM of about 8–10 ms (see below). The mammalian spark-like events shown in Fig. 2*Aa*–*c* had FDHM values of 35.7 (*a*), 46.5 (*b*) and 12.1 ms (*c*). The FDHM of events like those shown in *a*–*c* did not exceed 50 ms. As these ECRE displayed some morphological similarity to sparks of amphibian muscle but were not as stereotypical, we refer to this kind of mammalian event as spark-*like* events. However, a completely different type of ECRE could also be observed (Fig. 2*Ad*), featuring a steady or almost steady fluorescence level which could last for hundreds of milliseconds. The event shown in Fig. 2*Ad* had a FDHM of 336.2 ms. The FDHM for events with basically steady fluorescence levels throughout the event was always longer than 50 ms. Due to their duration and their appearance, we refer to this kind of event as ember-like. This is mainly for analogy with amphibian skeletal muscle, where the

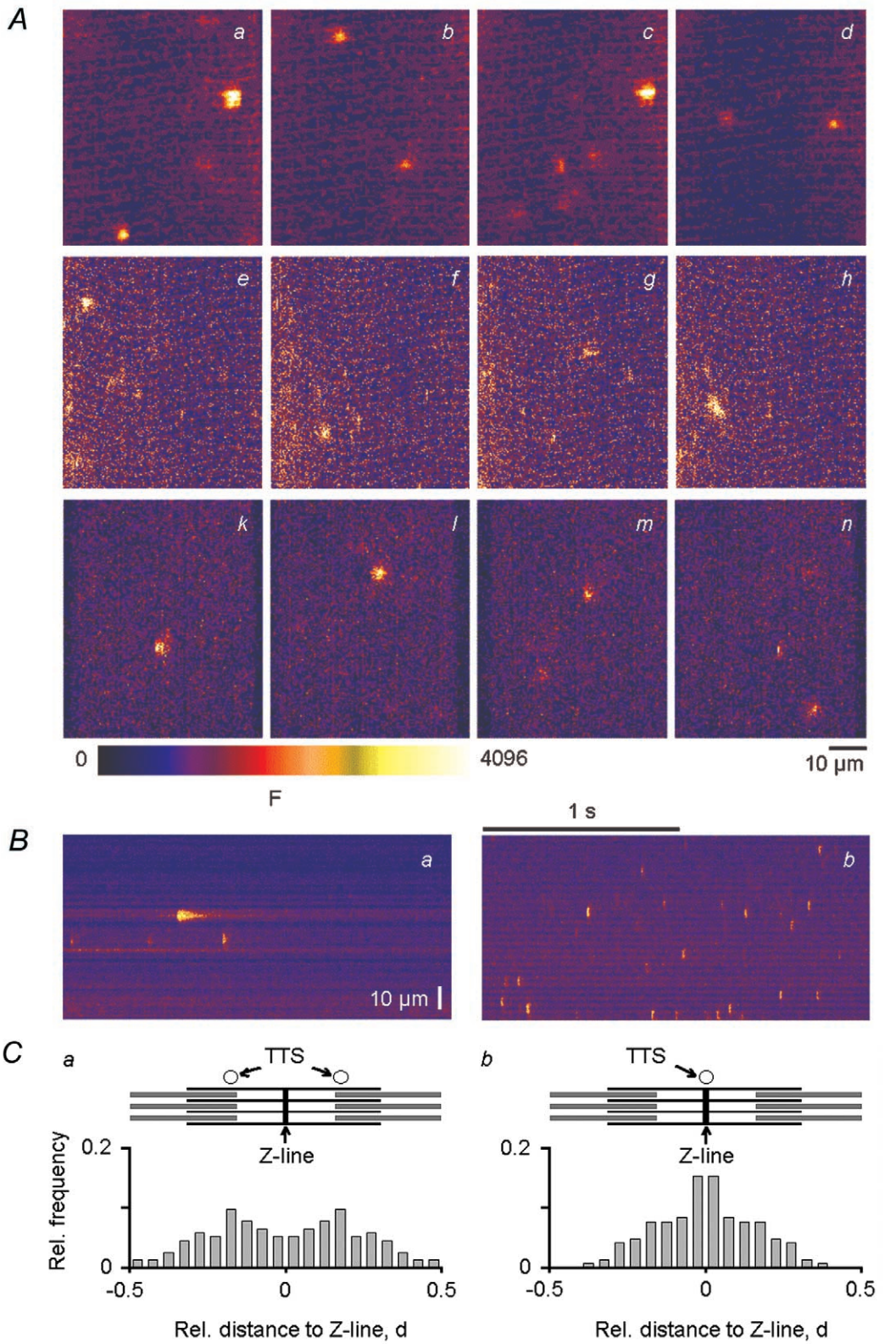

Figure 1. Elementary Ca^{2+} release events in adult mammalian skeletal muscle

A, consecutive x–y images of absolute fluorescence from a time series of 100 images (interval, 2 s) showing several discrete Ca^{2+} release events in a chemically (*a*–*d*) and a mechanically (*e*–*h*) skinned fibre from mouse and a chemically skinned fibre from rat (*k*–*n*). In all cases, the intracellular free Ca^{2+} and Mg^{2+} concentration was 100 nM and 0.6 mM, respectively. *B*, representative linescan images of absolute fluorescence from a chemically skinned fibre from mouse (*a*) and frog (*b*) muscle showing that the frequency of ECRE in mammalian muscle was about 1–3 per linescan image, compared with a frequency

term 'ember' is used to describe long-lasting prolongations (of the order of 50–100 ms) of individual sparks or spark averages, embers being interpreted as reflecting another event class for ECRE in E–C coupling (González *et al.* 2000*b*). In addition, events with combined features, containing spark-like and ember-like waveforms with steady fluorescence levels, also occurred (Fig. 2*Ae–g*). As a first simplifying approach for quantifying the different events containing ember-like time courses during our morphological analysis, we used the same algorithms for the determination of amplitude, FWHM, rise time and FDHM for all events, as given in Methods. The parameters for the events shown in Fig. 2*A* are given in the legend. It became clear that the amplitude and FWHM are fairly robust estimates for the events while the rise time depends greatly on the size and position of the spark-like component within the combined events. The most robust criterion for distinguishing spark-like from ember-like events in an all-event analysis turned out to be FDHM. We found it sufficient to define all ECRE with FDHM values less than 50 ms as spark-like and ECRE with FDHM values greater than 50 ms as ember-like. In addition to the thus defined 'pure' spark- and ember-like ECRE, 'combined ECRE' could be described by superposition of spark- and ember-like ECRE. These combined ECRE indicate that spark- and ember-like ECRE can occur in close proximity or that they may even be functionally connected.

The linescan in Fig. 2*B* shows that ECRE can also be evoked by depolarisation of the transverse tubular membrane in mechanically skinned fibre preparations. Replacement of the mammalian internal (high-K^+) solution with high-Na^+ solution resulted in a macroscopic Ca^{2+} transient. However, at the single triad level it was possible to resolve individual ECRE (red circles) within the global fluorescence increase, as shown in the four representative high-resolution lower panels of Fig. 2*B* that depict the time courses of normalised fluorescence for the locations marked by arrows. The more frequently individual events occurred at a certain location the faster was the rise of the absolute fluorescence signal, showing that the resolved ECRE contributed substantially to the overall Ca^{2+} increase. A close look at Fig. 2*B* revealed that most of the time a small increase in fluorescence could be noticed before a spark-like event occurred; this may be linked to preceding ember-like events that cannot be individually resolved within the macroscopic Ca^{2+} transient.

As ember-like events might be triggered via the DHPR, analogous to adult amphibian muscle where the ember was interpreted as directly voltage-operated release during voltage-clamp experiments, the frequency and morphology of ember-like events should be dependent on the state of the DHPR. The DHPR is exposed to a negative membrane potential in mechanically skinned fibres (e.g. Lamb & Stephenson, 1990) compared with a situation similar to a depolarised exterior membrane in chemically skinned fibres. A comparison of the parameter distributions, based on our methods, of all spontaneously occurring events for chemically skinned mammalian fibres (CSM, 5 fibres, $n = 465$), mechanically skinned mammalian fibres (MSM, 3 fibres, $n = 252$) and chemically skinned amphibian fibres (CSA, 4 fibres, $n = 258$) is shown in Fig. 3. The histograms for amplitude and FWHM were very similar for all three preparations, with some higher values for FWHM for mammalian fibres. The mean amplitude (F/F_0) was 1.91 ± 0.02 (CSA), 1.85 ± 0.01 (CSM) and 1.76 ± 0.01 (MSM), and the mean FWHM was 1.82 ± 0.03 μm (CSA), 1.87 ± 0.04 μm (CSM) and 2.12 ± 0.04 μm (MSM). In contrast there were distinct differences in the temporal parameters. The rise time and FDHM of amphibian Ca^{2+} sparks generally did not exceed 30 ms, with mean values of 5.81 ± 0.15 ms and 7.04 ± 0.16 ms, respectively. Therefore, in this preparation only spark-like events existed under our conditions using the above defined selection criterion, but no ember-like events (FDHM $>$ 50 ms). Comparable results were obtained in a previous study that described embers in amphibian muscle, where Ca^{2+} sparks but not embers were found in resting chemically skinned amphibian fibres (González *et al.* 2000*b*). For mechanically skinned mammalian fibres, the mean rise time was 17.5 ± 1.7 ms and the mean FDHM was 15.9 ± 1.5 ms. Surprisingly, in chemically skinned mammalian fibres the mean rise time and the mean FDHM were as high as 49.3 ± 3.4 and 48.2 ± 2.4 ms, respectively. In mechanically skinned mammalian fibres under our conditions, in contrast to resting chemically skinned amphibian fibres, a small but significant fraction (6 % of all events in Fig. 3) were ember-like events. An even larger fraction of ember-like events was observed in chemically skinned mammalian fibres (33 % of all events in Fig. 3). The difference in frequency of ember-like events in the two skinned mammalian fibre preparations may reflect different states of the DHPR–RYR complex connecting transverse tubular and SR membranes (see Discussion).

In addition to characterising the ECRE under resting conditions, we studied the effects of the RYR modulators caffeine and tetracaine, as well as those of variations of the free internal Mg^{2+} concentration, on the frequency of ECRE by *xyt*-series analysis, as described in Methods.

of about 10 events per linescan image in amphibian muscle. *C*, frequency histograms of the location of the ECRE maxima relative to the sarcomeric structure of skeletal muscle showing that ECRE mainly occurred at triadic junctions in both mammals (*a*) and frogs (*b*), because ECRE were most frequent at the expected locations of the transverse tubular system (TTS) of the respective species.

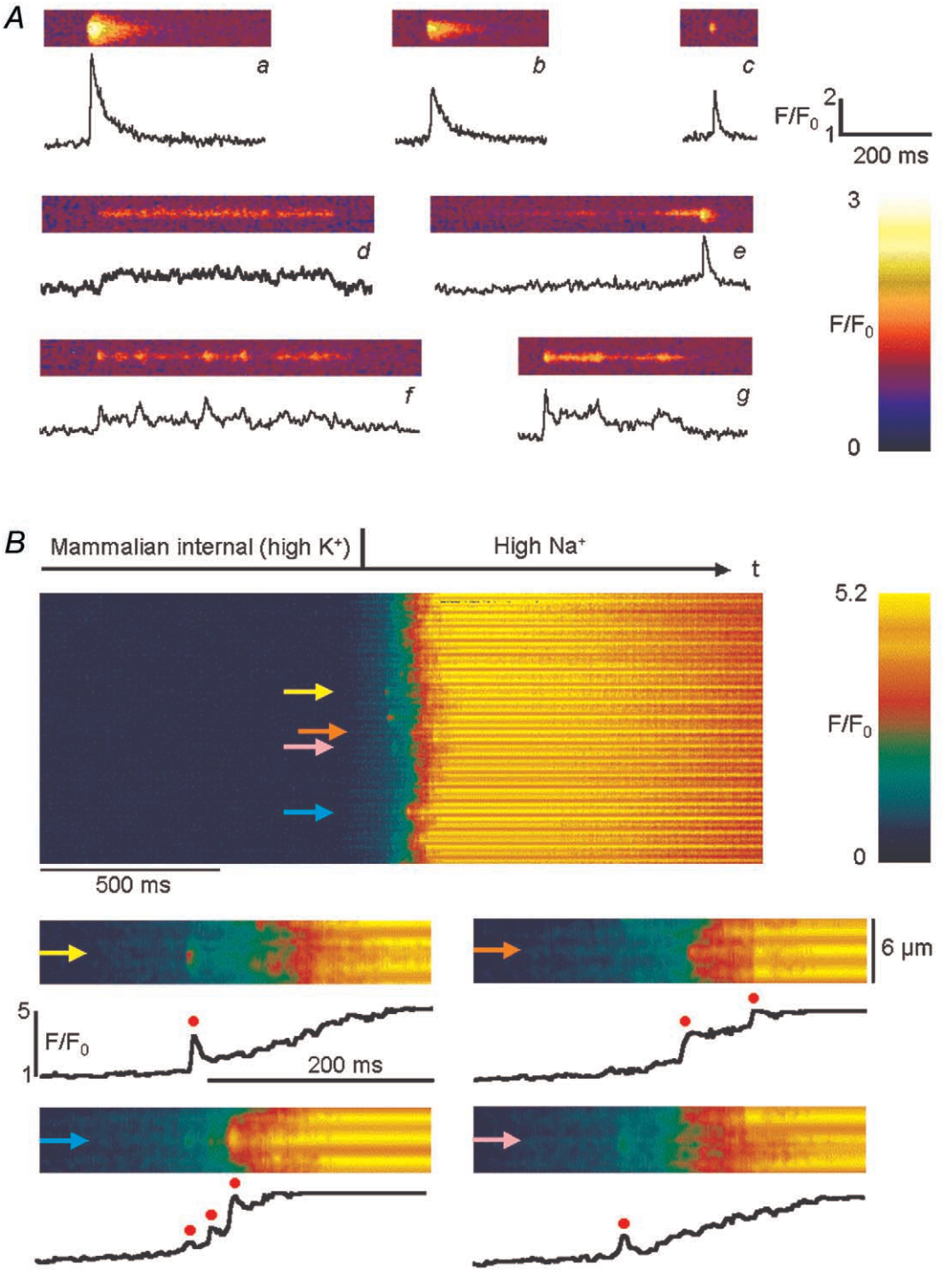

Figure 2. Linescan images of spontaneous and depolarisation-induced elementary Ca^{2+} release events

A, selected images (width, 10 μm) of normalised fluorescence showing the diversity of spontaneous ECRE in chemically or mechanically skinned mammalian fibres. The trace below each image shows the time course at the centre of the event. Short spark-like events (*a*–*c*) and long-lasting steady fluorescence events (ember-like events; *d*) coexisted with others that appeared to result from superposition of spark- and ember-like events (*e*–*g*). Morphological event parameter values for all events (amplitude (F/F_0), FWHM, rise time and FDHM, respectively) were: *a*: 3.57, 2.46 μm, 7.7 ms, 35.7 ms; *b*: 2.56, 3.4 μm, 16.9 ms, 46.5 ms; *c*: 2.51, 2.05 μm, 7.5 ms, 12.1 ms; *d*: 1.49, 1.5 μm, 256.1 ms, 336.2 ms; *e*: 2.54, 3.0 μm, 17.3 ms, 43.6 ms; *f*: 2.14, 1.91 μm, 15.9 ms, 79.9 ms; and *g*: 2.48, 1.91 μm, 5.85 ms, 80.8 ms. *B*, Ca^{2+} release induced by depolarisation following replacement of the mammalian internal (high-K^+) solution with high-Na^+ internal solution in a mechanically skinned fibre. Lower panels: 4 high-resolution images with representative time courses (marked by arrows) showing that individual ECRE (red circles) can be resolved within the global fluorescence signal at the single triad level.

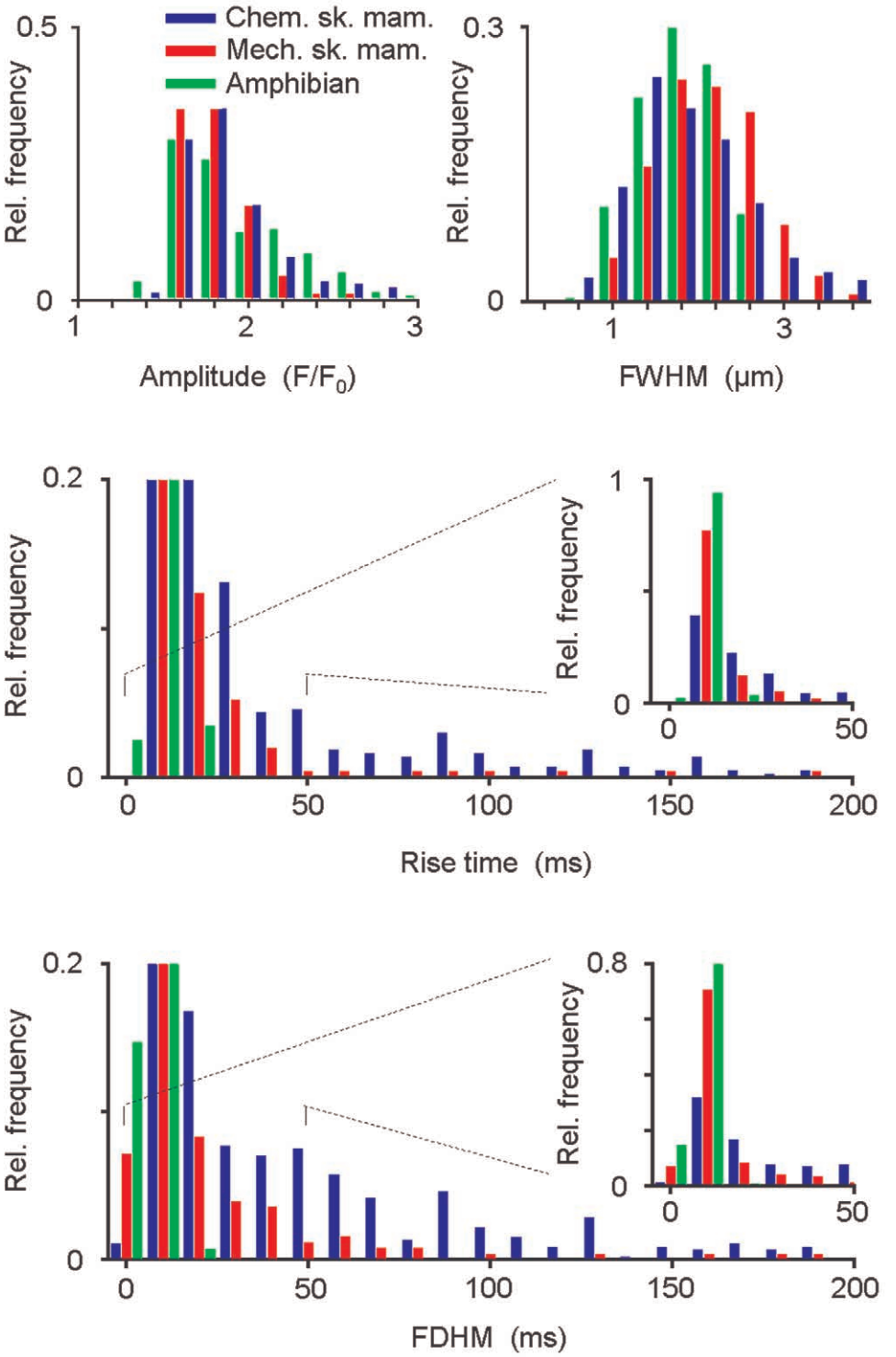

Figure 3. Morphological event parameters of resting skinned fibres in amphibian and mammalian muscle

Normalised frequency histograms showing the distribution of the four morphological parameters, amplitude, FWHM, rise time and FDHM, of all events in chemically skinned amphibian fibres (green), mechanically skinned mammalian fibres (red) and chemically skinned mammalian fibres (blue). The most remarkable differences were in the rise time and FDHM. The ordinates of the histograms for these temporal parameters were scaled so that events with a long rise time or FDHM could be adequately seen. The histograms shown in the insets display the subset of events for parameter values smaller than 50 ms on the full ordinate scale. The amphibian event set contained no ember-like events (defined as FDHM $>$ 50 ms). In mechanically and chemically skinned mammalian fibres, respectively, 6 % and 33 % of all events were ember-like.

Figure 4*A* shows that a significant overall increase in event frequency of 176% was observed in a representative chemically skinned mammalian fibre upon application of 0.5 mM caffeine. On average, the increase in event frequency was 225 ± 14% for three studied fibres ($P < 0.05$ in all cases). Similar effects were found in amphibians; a representative fibre is shown in the lower panel of Fig. 4*A* where the event frequency increased by

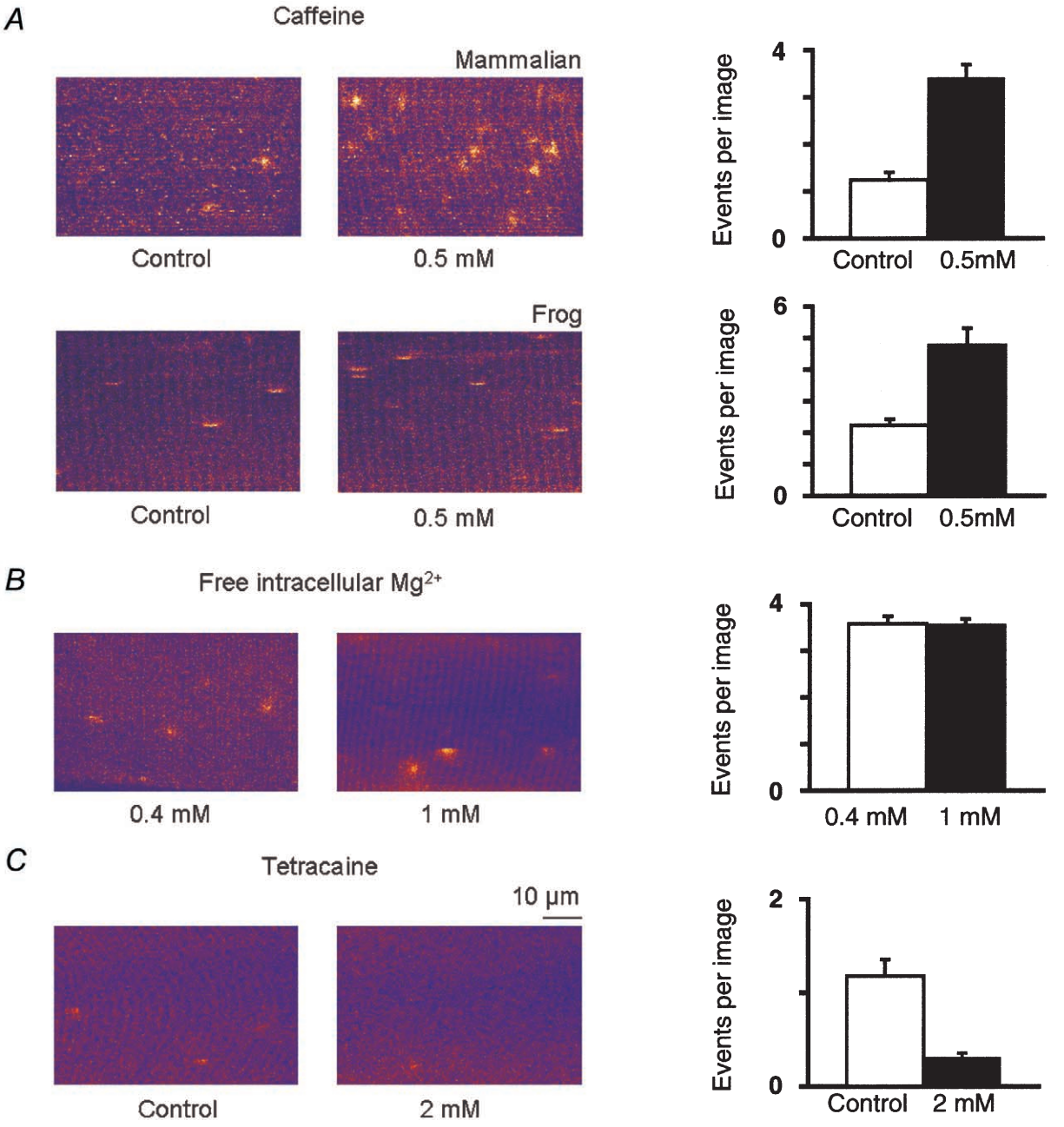

Figure 4. Modulation of ECRE frequency in adult mammalian muscle

In *A*, the effect of 0.5 mM caffeine on the event frequency in a chemically skinned mammalian and a chemically skinned amphibian fibre is demonstrated in two representative x–y images (70 μm × 50 μm). The mean number of events per image in a *xyt*-series in these two representative fibres increased from 1.24 ± 0.17 (20 images, mammalian) and 2.23 ± 0.19 (50 images, amphibian) under control conditions to 3.42 ± 0.28 (80 images, mammalian) and 4.78 ± 0.53 (50 images, amphibian) in the presence of caffeine. *B*, the frequency of ECRE observed in a representative chemically skinned mammalian fibre exposed to a free intracellular Mg^{2+} concentration of 0.4 mM (3.58 ± 0.16 events per image, 100 images) was comparable with that observed in a chemically skinned mammalian fibre in 1 mM free Mg^{2+} (3.54 ± 0.14 events per image, 100 images), showing that 1 mM free intracellular Mg^{2+} was not a limiting factor for the observation of ECRE in skinned fibres. *C*, the frequency of ECRE was reduced from 1.18 ± 0.18 (100 images) to 0.31 ± 0.05 (100 images) upon application of 2 mM tetracaine in a representative chemically skinned mammalian fibre.

114%. This indicates that ECRE originate from RYRs and supports the view that ECRE can be modulated by Ca^{2+} and CICR in adult mammalian and frog skeletal muscle. The intracellular free Mg^{2+} concentration was found not to be a limiting factor for ECRE production in adult mammalian skeletal muscle, as ECRE were readily detected at free Mg^{2+} concentrations ranging from 0.4 to 1 mM. A comparison of two representative chemically skinned mammalian fibres observed in 0.4 mM Mg^{2+} and 1 mM Mg^{2+}, showing that the frequency of ECRE in 1 mM Mg^{2+} was similar to that in 0.4 mM Mg^{2+}, is shown in Fig. 4*B*. We found a frequent occurrence of ECRE in all chemically skinned fibres studied in 1 mM Mg^{2+}; on average the frequency of ECRE in 1 mM Mg^{2+} (3 fibres) did not differ significantly from that in 0.4 mM Mg^{2+} (3 fibres, $P > 0.05$). Both event types of ECRE, spark- and ember-like, could still be observed 2 min after exposure of the fibres to 200 μM or 2 mM tetracaine, as studied by line scanning. A concentration of tetracaine of 200 μM did not significantly reduce the frequency of ECRE under our conditions (3 fibres, $P > 0.05$), and even the application of 2 mM tetracaine did not completely inhibit ECRE, as shown in Fig. 4*C* for a chemically skinned mammalian fibre. On average, 2 mM tetracaine significantly reduced the frequency of ECRE by 74 ± 15% (2 fibres, $P < 0.05$). It is also interesting that we did not find a specific and complete inhibition of either spark- or ember-like events.

DISCUSSION

We have unequivocally shown that abundant elementary Ca^{2+} release events (ECRE) exist in chemically as well as in mechanically skinned fibres from fast-twitch EDL muscle of adult mammals. To date there has been disagreement in the field as to whether abundant ECRE can be resolved in adult mammalian skeletal muscle. The ECRE found in this study may provide the basis for mammalian skeletal muscle Ca^{2+} release and E–C coupling. Mammalian ECRE originate mainly at the triadic junctions and can occur spontaneously or be evoked by depolarisation. Therefore very similar mechanisms to those in amphibian muscle or developing mammalian muscle should participate in the event generation. A further similarity between amphibian and mammalian muscle is the increase in frequency of ECRE following application of low concentrations of caffeine, as demonstrated in this study. This supports the idea that Ca^{2+} and CICR are involved in the production of adult mammalian muscle ECRE, although the exact mechanism of caffeine action is still unclear (Herrmann-Frank *et al.* 1999). In this context, it should be noted that caffeine has also been shown to shift the transfer function of charge movement associated with DHPR activation (Shirokova & Ríos, 1996) and may additionally modify the interaction between the DHPR and RYR.

In addition to the existence of ECRE, we have identified two basic event types based on the morphology of ECRE in permeabilised fibres of adult mammalian muscle. Both fundamental Ca^{2+} release types, spark- and ember-like events, occur individually and in superposition in resting skinned mammalian fibres, whereas in chemically skinned frog fibres only Ca^{2+} sparks are detected.

The contribution of individual events to a global fluorescence signal (Fig. 2*B*) supports the idea that global Ca^{2+} transients involve the superposition of many ECRE. Initial small increases in fluorescence may be due to ember-like events preceding the individually resolved spark-like events within depolarisation-induced Ca^{2+} transients. However, as the rise time and FDHM of the mammalian ECRE are considerably longer than those in amphibians it is unlikely that global mammalian Ca^{2+} release can be explained solely by superposition of these events without the assumption of further control factors.

In our study, ECRE in chemically skinned fibres included a greater number of ember-like events than that in mechanically skinned fibres. In mechanically skinned fibres the DHPRs 'face' a membrane potential in the resealed transverse tubules (Lamb & Stephenson, 1990), whereas the state of the DHPR in chemically skinned fibres is less defined and the exterior membrane is completely depolarised. As this is the foremost difference between these two preparations the morphological event parameters suggest that the occurrence of spontaneous ember-like events may reflect an interaction of the DHPR with the RYR that is somewhat uncoupled either by the chemical skinning process itself or the resulting depolarisation of the transverse tubules. A very tight control of the state of the DHPR–RYR complex by membrane voltage in mammalian muscle could, at least in part, explain why we only rarely observed ECRE in completely intact fibres (W. G. Kirsch, unpublished observation) with stable resting potentials, in agreement with Conklin *et al.* (1999), or why ECRE have not been observed in cut mammalian fibres under voltage-clamp conditions (Shirokova *et al.* 1998). For the above reasons we have termed the observed mammalian long-duration event type ember-like, by analogy to embers in amphibian muscle.

It should be pointed out that spark- and ember-like events can occur at the same site (combined events), which would suggest a coupling of two or more closely located release sites or different control mechanisms for the various parts of the same release site, or both. At least a duality of control mechanisms for the triadic junction is expected from the skip pattern, suggesting a possible interplay of RYRs colocalised and not colocalised with DHPRs. Furthermore, a multiplicity of additional control factors for Ca^{2+} release like calmodulin, FKBP12, redox state of the DHP–RYR complex, Ca^{2+} in the SR, or others may exist.

It is interesting to note that a free Mg^{2+} concentration of 1 mM did not strongly inhibit ECRE in chemically

skinned fibres of adult mammalian muscle, as expected from other studies (Fink & Stephenson, 1987; Lacampagne *et al.* 1998). Therefore, a free Mg^{2+} concentration around 1 mM is unlikely to be the reason for the scarce occurrence of ECRE in intact fibres. This scarcity can rather be explained by a greater control of the RyR by the DHPR during ECRE in mammalian compared with amphibian muscle (see also Shirokova *et al.* 1998, 1999). We have shown that tetracaine acts as an inhibiting factor for ECRE only at substantially higher concentrations (2 mM) than in amphibian skeletal muscle. Even a concentration of tetracaine of 2 mM did not completely inhibit either spark-like or ember-like ECRE in adult mammalian muscle, whereas 200 μM is apparently enough to completely eliminate Ca^{2+} sparks in experiments with cut fibres from amphibian muscle (Shirokova & Ríos, 1997). Differential effects for concentrations of tetracaine lower than 1.25 mM, with possibly higher ECRE frequencies than in control conditions due to a higher Ca^{2+} content of the SR, have been reported in mammalian heart muscle (Györke *et al.* 1997; Smith & O'Neill, 2001). The difference in tetracaine sensitivity between amphibian and mammalian skeletal muscle may be a further indication that additional control factors are involved in the generation of ECRE in adult mammalian compared with amphibian skeletal muscle.

In conclusion, we have presented here unequivocal evidence for the existence of ECRE in adult mammalian muscle, consisting of ember-like, spark-like and combined events. Based on these findings, our experimental approach should allow further studies to elucidate which of the known or still unknown control factors, in addition to membrane potential, govern ECRE and regulate the underlying functional molecular mechanisms which are of central importance for excitation–contraction coupling in mammalian muscle.

Balshaw, D. M., Xu, L., Yamaguchi, N., Pasek, D. A. & Meissner, G. (2001). Calmodulin binding and inhibition of cardiac muscle calcium release channel (ryanodine receptor). *Journal of Biological Chemistry* **276**, 20144–20153.

Block, B. A., Imagawa, T., Campbell, K. P. & Franzini-Armstrong, C. (1988). Structural evidence for direct interaction between the molecular components of the transverse tubule/sarcoplasmic reticulum junction in skeletal muscle. *Journal of Cell Biology* **107**, 2587–2600.

Cheng, H., Lederer, W. J. & Cannell, M. B. (1993). Calcium sparks: elementary events underlying excitation-contraction coupling in heart muscle. *Science* **262**, 740–744.

Conklin, M. W., Ahern, C. A., Vallejo, P., Sorrentino, V., Takeshima, H. & Coronado, R. (2000). Comparison of Ca^{2+} sparks produced independently by two ryanodine receptor isoforms (type 1 or type 3). *Biophysical Journal* **78**, 1777–1785.

Conklin, M. W., Barone, V., Sorrentino, V. & Coronado, R. (1999). Contribution of ryanodine receptor type 3 to Ca^{2+} sparks in embryonic mouse skeletal muscle. *Biophysical Journal* **77**, 1394–1403.

Dulhunty, A. F. (1992). The voltage-activation of contraction in skeletal muscle. *Progress in Biophysics and Molecular Biology* **57**, 181–223.

Escobar, A. L., Monck, J. R., Fernandez, J. M. & Vergara, J. L. (1994). Localization of the site of Ca^{2+} release at the level of a single sarcomere in skeletal muscle fibres. *Nature* **367**, 739–741.

Fink, R. H. A. & Stephenson, D. G. (1987). Ca^{2+}-movements in muscle modulated by the state of K^+-channels in the sarcoplasmic reticulum membrane. *Pflügers Archiv* **409**, 374–380.

Franzini-Armstrong, C. & Protasi, F. (1997). Ryanodine receptors of striated muscles: a complex channel capable of multiple interactions. *Physiological Reviews* **77**, 699–729.

González, A., Kirsch, W. G., Shirokova, N., Pizarro, G., Brum, G., Pessah, I. N., Stern, M. D., Cheng, H. & Ríos, E. (2000*a*). Involvement of multiple intracellular release channels in calcium sparks of skeletal muscle. *Proceedings of the National Academy of Sciences of the USA* **97**, 4380–4385.

González, A., Kirsch, W. G., Shirokova, N., Pizarro, G., Stern, M. D. & Ríos, E. (2000*b*). The spark and its ember: separately gated local components of Ca^{2+} release in skeletal muscle. *Journal of General Physiology* **115**, 139–158.

Györke, S., Lukyanenko, V. & Györke, I. (1997). Dual effects of tetracaine on spontaneous calcium release in rat ventricular myocytes. *Journal of Physiology* **500**, 297–309.

Haarmann, C., Fink, R. H. A. & Dulhunty, A. F. (1999). Oxidation and reduction of pig skeletal muscle ryanodine receptors. *Biophysical Journal* **77**, 3010–3022.

Herrmann-Frank, A., Luttgau, H. C. & Stephenson, D. G. (1999). Caffeine and excitation-contraction coupling in skeletal muscle: a stimulating story. *Journal of Muscle Research and Cell Motility* **20**, 223–237.

Klein, M. G., Cheng, H., Santana, L. F., Jiang, Y. H., Lederer, W. J. & Schneider, M. F. (1996). Two mechanisms of quantized calcium release in skeletal muscle. *Nature* **379**, 455–458.

Lacampagne, A., Klein, M. G. & Schneider, M. F. (1998). Modulation of the frequency of spontaneous sarcoplasmic reticulum Ca^{2+} release events (Ca^{2+} sparks) by myoplasmic [Mg^{2+}] in frog skeletal muscle. *Journal of General Physiology* **111**, 207–224.

Lamb, G. D. (2000). Excitation-contraction coupling in skeletal muscle: comparisons with cardiac muscle. *Clinical and Experimental Pharmacology and Physiology* **27**, 216–224.

Lamb, G. D. & Stephenson, D. G. (1990). Calcium release in skinned muscle fibres of the toad by transverse tubule depolarization or by direct stimulation. *Journal of Physiology* **423**, 495–517.

Lipp, P. & Niggli, E. (1998). Fundamental calcium release events revealed by two-photon excitation photolysis of caged calcium in guinea-pig cardiac myocytes. *Journal of Physiology* **508**, 801–809.

Nelson, M. T., Cheng, H., Rubart, M., Santana, L. F., Bonev, A. D., Knot, H. J. & Lederer, W. J. (1995). Relaxation of arterial smooth muscle by calcium sparks. *Science* **270**, 633–637.

Ríos, E. & Brum, G. (1987). Involvement of dihydropyridine receptors in excitation-contraction coupling in skeletal muscle. *Nature* **325**, 717–720.

Shirokova, N., García, J. & Ríos, E. (1998). Local calcium release in mammalian skeletal muscle. *Journal of Physiology* **512**, 377–384.

Shirokova, N. & Ríos, E. (1996). Caffeine enhances intramembranous charge movement in frog skeletal muscle by increasing cytoplasmic Ca^{2+} concentration. *Journal of Physiology* **493**, 341–356.

Shirokova, N. & Ríos, E. (1997). Small event Ca^{2+} release: a probable precursor of Ca^{2+} sparks in frog skeletal muscle. *Journal of Physiology* **502**, 3–11.

Shirokova, N., Shirokov, R., Rossi, D., González, A., Kirsch, W. G., García, J., Sorrentino, V. & Ríos, E. (1999). Spatially segregated control of Ca^{2+} release in developing skeletal muscle of mice. *Journal of Physiology* **521**, 483–495.

Smith, G. L. & O'Neill, S. C. (2001). A comparison of the effects of ATP and tetracaine on spontaneous Ca^{2+} release from rat permeabilised cardiac myocytes. *Journal of Physiology* **534**, 37–47.

Smith, R. M. & Martell, A. E. (1994). *Critical Stability Constants*. Plenum Press, New York.

Tsugorka, A., Ríos, E. & Blatter, L. (1995). Imaging elementary events of calcium release in skeletal muscle cells. *Science* **269**, 1723–1726.

Uttenweiler, D., Weber, C. & Fink, R. H. A. (1998). Mathematical modelling and fluorescence imaging as a new approach to study the Ca^{2+}-turnover in skinned muscle fibres. *Biophysical Journal* **74**, 1640–1653.

Ward, C. W., Schneider, M. F., Castillo, D., Protasi, F., Wang, Y., Chen, S. R. W. & Allen, P. D. (2000). Expression of ryanodine receptor RyR3 produces Ca^{2+} sparks in dyspedic myotubes. *Journal of Physiology* **525**, 91–103.

Acknowledgements

We thank Dr E. Ríos and Dr A. González for helpful discussions and comments. This study was supported by DFG FOR 240/3-1 and BMBF 13N7871.

W. G. Kirsch and D. Uttenweiler contributed equally to this work.

Corresponding author

R. H. A. Fink: Institute of Physiology and Pathophysiology, Medical Biophysics, University of Heidelberg, Im Neuenheimer Feld 326, 69120 Heidelberg, Germany.

Email: rainer.fink@urz.uni-heidelberg.de